Characterization of Temperature Profile in Furnace and Solubility of Iron in Silicon

by

Vrajesh Y. Modi

SUBMITTED TO THE DEPARTMENT OF MECHANICAL ENGINEERING
IN PARTIAL FULFILLMENT OF THE REQUIREMENTS FOR THE
DEGREE OF

BACHELOR OF SCIENCE IN MECHANICAL ENGINEERING

AT THE

MASSACHUSETTS INSTITUTE OF TECHNOLOGY

JUNE 2011

Signature of Author: _____
Department of Mechanical Engineering
January 27, 2011

Certified by: _____
Tonio Buonassisi
Assistant Professor of Mechanical Engineering
Thesis Supervisor

Accepted by: _____
John H. Lienhard V
Samuel C. Collins Professor of Mechanical Engineering
Undergraduate Officer

Characterization of Temperature Profile in Furnace and Solubility of Iron in Silicon

by

Vrajesh Y. Modi

Submitted to the Department of Mechanical Engineering
on January 27, 2011 in Partial Fulfillment of the
Requirements for the Degree of Bachelor of Science in
Mechanical Engineering

ABSTRACT

A better understanding of the behavior of impurities, such as iron, in silicon can lead to increases in solar cell efficiency. The purpose of this thesis was to study the behavior of iron in silicon via three sub-tasks: (a) to determine an appropriate dwell time, characterize the temperature profile within a vertical high-temperature tube furnace as a function of depth and flow rate, (b) to use this information to diffuse iron into silicon at a known temperature, and (c) to measure the in-diffused iron concentration by comparing minority carrier lifetime measurements before and after iron-boron pair (Fe_i-B_s) dissociation. For the thermocouple used, a furnace dwell time of 15 minutes was determined to be sufficient to reach a stable temperature. At a forming gas flow rate of 1.0 SCFM, the ratio of the temperature in the furnace to the set temperature, θ, as a function of depth in inches, d, is described by the equation $\theta = -7.29\times10^{-4}\cdot d^2 + 0.0177\cdot d + 0.897$. The effect of varying the flow rate on the temperature profile was minor, and, depending on the application, negligible. There was a great deal of variance in the measured iron concentrations in the samples, suggesting that improvements to the procedure would yield more consistent results. Possible sources of error included presence of other metastable defects (in addition to Fe_i-B_s / Fe_i), surface recombination, and high sensitivity of the calculated iron concentration to the measured minority carrier lifetimes.

Thesis Supervisor: Tonio Buonassisi
Title: Assistant Professor of Mechanical Engineering

1. Introduction

Efficiency of solar photovoltaic cells is affected by the presence of impurities. A better understanding of the kinetics of these impurities during thermal processing could lead to increases in solar cell efficiency, which would increase their desirability as an energy source. Multicrystalline silicon (mc-Si) is widely used due to financial considerations, although it contains high levels of impurities, because monocrystalline silicon, which is currently used in the semiconductor industry, is energy-intensive to produce and expensive for use in solar cells. Existing experimental data for the diffusivities of certain metals in silicon vary by orders of magnitude, so there is a need for more reliable data to accurately simulate the evolution of metals in mc-Si during solar cell processing.

The goal of this thesis was two-fold: (1) to determine an appropriate dwell time and then characterize the temperature profile within a furnace capable of heating silicon to high temperatures, and (2) to use said furnace to quantify the solubility of iron in silicon. While this thesis did not measure diffusivity directly, it did examine the repeatability of carrier lifetimes for a particular approach. For furnace calibration, variables that were considered included position within the furnace and gas flow rate.

Section 2 of this thesis discusses the theory behind heat transfer and solubility; it also provides a brief overview of the equipment. Section 3 examines in greater depth the experimental setup and the methods used to make the measurements. Section 4 discusses the findings and compares them to expected data. Section 5 explores the implications and recommends areas that merit further investigation.

2. Theory

An understanding of the basic heat and mass transfer mechanisms and fundamentals of the instrumentation is helpful in evaluating the methods and results. This section briefly recaps these topics; more detailed discussion is available by consulting the references.

2.1 Heat Transfer[1]

There exist three modes of heat transfer: conduction, convection, and radiation. In this paper, we concern ourselves with convection and with radiation; since there is minimal direct contact between the sample and the sides of the furnace, we ignore heat transfer due to conduction.

Convection is governed by Newton's Law of Cooling, where the heat flux from the surface, q, is equal to the difference between the temperatures of the surface, T_s, and gas, T_∞, times the surface area, A, times h, the convective heat transfer coefficient:

$$q = hA(T_s - T_\infty) \quad (1)$$

Radiation is governed by the Stefan-Boltzmann law; the resulting equation takes a similar form, where the heat flux from the surface, q, is equal to the emissivity of the surface, ε, times the area, A, times the Stefan-Boltzmann constant, σ, times the difference of the fourth powers of the temperatures of the surface, T_s, and its surroundings, T_{sur}:

$$q = \varepsilon A\sigma(T_s^4 - T_{sur}^4) \quad (2)$$

The value of the Stefan-Boltzmann constant is 5.67×10^{-8} W/(m^2·K^4). The emissivity of alumina at 1000K is 0.33.[1] Note that the same surface may simultaneously transfer heat by convection and by radiation; in this case, we simply add the contributions of each.

2.2 Behavior of Iron in Silicon

Diffusion of iron into silicon is governed by Fick's law.[1] In this experiment, the silicon sample was coated with an excess of iron, and then held at a high temperature for a long enough period of time that the silicon was saturated with iron. Quenching the sample allows the silicon to contain a much higher concentration of iron at room temperature than the equilibrium concentration.

The presence of iron-boron pairs in silicon is known to greatly shorten the carrier lifetime; given the doping level of the silicon and the specified minority carrier density, we expect that the carrier lifetime will be increased when these pairs are dissociated.[2]

2.3 Carbolite Furnace

The procedure described in section 3 was, in large part, carried out using a vertical tube furnace (Figure 1). The furnace contained six silicon carbide heating elements surrounded by insulation.[3] An alumina tube, capable of withstanding high temperatures, went through the center of the furnace to prevent direct contact between the heating elements and the samples. A programmable temperature controller used feedback from a built-in thermocouple to adjust the furnace temperature to the desired temperature. However, the thermocouple was located near the

heating elements outside the alumina tube, while the quantity of interest was the temperature at a particular depth at the center of the tube, where the samples would be heated.

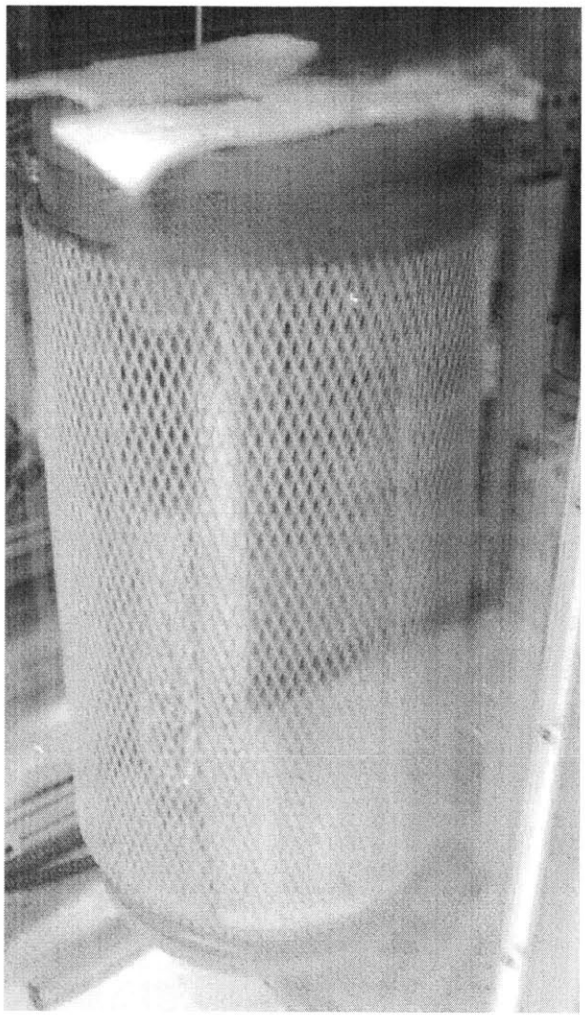

Figure 1: This Carbolite vertical tube furnace was used to heat the samples to the desired temperatures. The goal of the first part of the procedure was to accurately describe the temperature profile within this furnace.

2.4 Type R Thermocouple

To determine the temperature at the position of interest, a 24-inch Omega Type R thermocouple was used (Figure 2). The thermocouple, which produced a voltage difference as a function of temperature, was connected to a junction box, which provided a digital readout to a computer. The computer recorded the digital readout, and the set temperatures, which were programmed directly into the furnace temperature controller, were added to relevant plots afterwards.

Figure 2: A 24-inch Omega Type R thermocouple was used to measure the temperature inside the furnace. The probe was made of a platinum-rhodium alloy.[4]

2.5 Silicon Wafer Lifetime Tester

In the final section of the procedure, the minority carrier lifetimes in the samples were measured using a silicon wafer lifetime tester (Figure 3) known as a quasi-steady-state photoconductivity (QSSPC) measurement device. Since the silicon samples were p-type, there was boron in the samples. In the dark, iron formed a coulombic pair with the boron, while in light, all iron was interstitial since the bond energy was exceeded.

The tester produced flashes of light, which injected carriers (electrons and holes) into the sample. The resulting Eddy currents induced a current in the device, which was measured to determine the minority carrier lifetimes.[5]

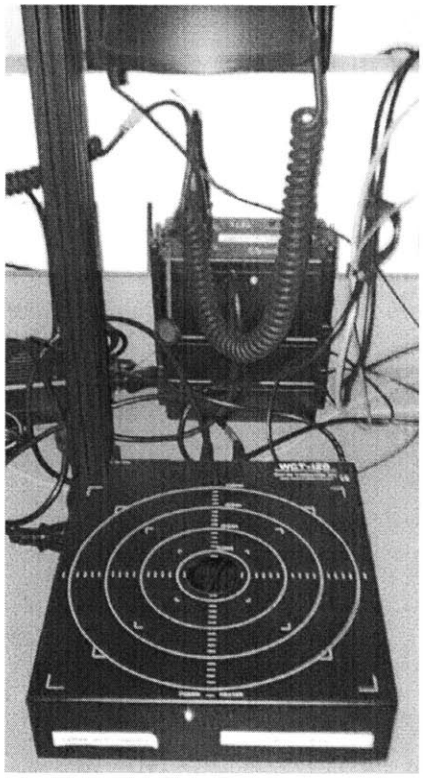

Figure 3: A silicon wafer carrier lifetime tester was used to measure the lifetime of the carriers (electrons and holes) in the samples. This was used to determine the concentration of iron present.

3. Methods

The experimental procedure can be divided into five distinct phases. First, an appropriate dwell time for the furnace was determined to enable accurate temperature measurements based on the time constant of the thermocouple. Second, the thermocouple was used to measure the temperature profile in the furnace at different depths and at different flow rates. Third, samples of silicon with an iron surface coating were placed in the furnace to allow the iron to diffuse into the silicon, and then they were quenched. Fourth, a number of steps were taken to clean the samples and prepare them for the final step. Fifth, the minority carrier lifetimes were measured before and after illumination, from which iron-boron pair concentrations were calculated.

3.1 Determination of Dwell Time

Given that the thermocouple was known to have a long time constant (several minutes), it was necessary to hold the temperature of the furnace steady for a certain period of time to make an accurate temperature measurement. The first step, of the procedure, then, was to determine an appropriate dwell time so that the later parts of the procedure could be run as efficiently as possible. The dwell time was the amount of time that the set temperature of the furnace would need to be held constant at a given temperature to allow the thermocouple to "catch up"; this would ensure an accurate reading of the temperature inside the furnace at a given depth at that set temperature.

To determine the optimal dwell time, the furnace was ramped (at 5°C/min to avoid excessive thermal stress) to 900°C, 1000°C, 1100°C, and 1200°C, and the response from the thermocouple was recorded. During this phase, a dwell time of 30 minutes was used, since this was known to substantially exceed the optimal dwell time based on past experience. An appropriate dwell time was determined by inspection from the plot, based on the amount of time that it took the thermocouple trace to become steady after the furnace had reached a new set temperature.

3.2 Measurement of Temperature

The first major goal of this thesis was to characterize the temperature profile inside the furnace as a function of depth and flow rate; three different approaches were taken. First, the thermocouple was held at a constant depth, and the set temperature of the furnace was varied. Second, the set temperature of the furnace was held fixed, and the depth of the thermocouple was

varied. Third, to determine the effect of changes to flow rate, the depth and set temperature of the furnace were held constant, and the flow rate was varied.

For future experimentation, the second method (temperature fixed, depth varied) is recommended because it is faster and because it produces more accurate results due to less variation in gas flow rate and sensor positioning. The main drawback is that without an automated way to adjust the depth of the thermocouple, the setup requires constant attention since the depth of the thermocouple needs to be adjusted every 15 minutes. In contrast, the first method (depth fixed, temperature varied) can be carried out with minimal human attention due to the programmable nature of the furnace.

3.3 Quenching Silicon Samples

The second major goal of this thesis was to quantify the diffusion of iron into silicon. In this experiment, samples were produced at two different temperatures, 766°C, and 845°C. In both cases, a 150 nm coating of iron was applied to a 310 μm thick sample of silicon (Czochralski process, doping level 1×10^{14} cm^{-3}), which was a 1.5 inch diameter disk. Then, the sample was placed onto a quartz sample holder and carefully lowered into the preheated furnace to a depth of 14 inches below the top of the furnace, which was determined to be the appropriate depth to obtain the desired temperature based on the results of the previous section. Nitrogen gas was flowed through the tube at a rate of 1.0 SCFM to avoid oxidation of the sample at the high temperature. The sample was held at the prespecified temperature for the appropriate amount of time, 75 minutes for 766°C, and 45 minutes for 845°C. This provided plenty of time for iron to diffuse into the silicon sample and saturate it at that particular temperature. Then, the gas flow was disconnected and the sample was immediately shaken off of the sample holder into a beaker of silicone oil at room temperature, causing the sample to be quenched before the iron had a chance to diffuse back out. This setup is illustrated in Figure 4.

Unfortunately, the samples that were heated to 845°C repeatedly shattered upon hitting the oil, likely due to the thermal stresses that were induced. The equipment used in the measurement of carrier lifetime, described in section 3.5, requires the samples be no smaller than 1.5 inches in diameter, so smaller samples would not be a feasible workaround unless different equipment is used for the carrier lifetime measurement. Another possible workaround would be to heat the oil above room temperature to reduce the thermal stress during quenching.

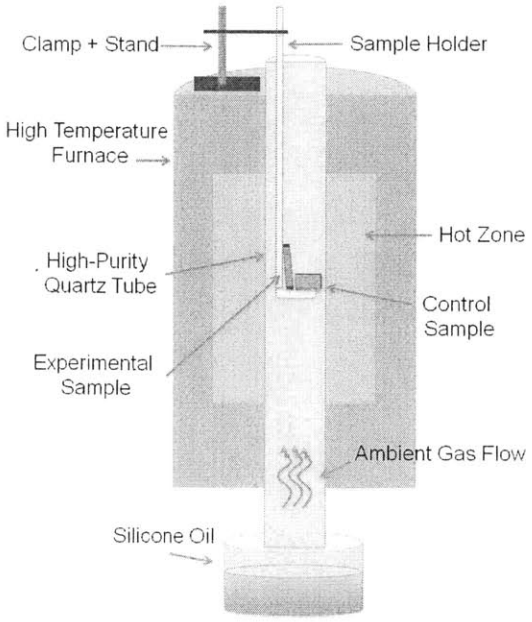

Figure 4: This schematic represents the experimental setup during the quenching phase. Note that the gas flow was disconnected and the end cap removed immediately before the sample was dropped into the oil to quench it. Schematic courtesy of David Fenning.

3.4 Further Processing of Samples

After being quenched, samples were rinsed in a sonicator, first using acetone and then using water. Next, the samples were polished using 800 grit sandpaper, then 1200 grit sandpaper, then 3 μm diamond paste. This produced a very smooth surface, on which silicon nitride was deposited. These steps prepared the samples for the final phase of the experiment.

3.5 Measurement of Carrier Lifetime

In the experiment's final phase, the carrier lifetimes of the samples were measured ten times (five on each side). Then, each sample was placed under a 1kW halogen lamp for ten minutes (Figure 5), to dissociate the Fe-B bonds, and then the carrier lifetimes were measured again.

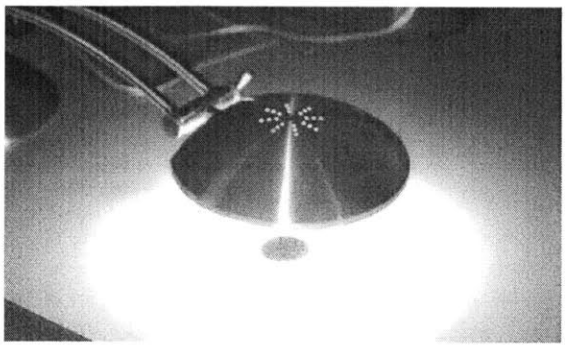

Figure 5: A 1kW halogen lamp was used to dissociate the Fe-B bonds. Samples were placed under the lamp for ten minutes before their carrier lifetime was measured again.

4. Results and Discussion

Fifteen minutes was determined to be a sufficient dwell time. At a flow rate of 1.0 SCFM, the ratio of the temperature in the furnace to the set temperature, θ, as a function of depth in inches, d, was described well by the equation

$$\theta = (-7.29 \times 10^{-4})d^2 + 0.0177d + 0.897. \quad (3)$$

Note that all temperatures were measured in Kelvin. The flow rates allowed by the equipment used (up to 5.0 SCFM) had a negligible effect on the temperature inside the furnace. Process abnormalities led to inconsistent results for the carrier lifetimes of the tested samples. The following subsections describe each of these results in greater detail.

4.1 Dwell Time

By inspection, it was determined that a dwell time of fifteen minutes would be sufficient to have a steady reading on the thermocouple for a given set temperature. This dwell time was used for all successive runs. The results are shown in Figure 6.

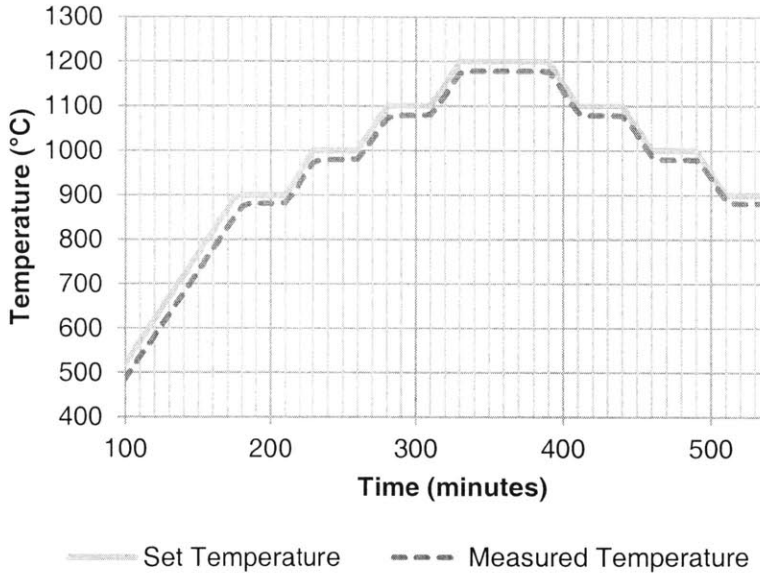

Figure 6: A dwell time of 30 minutes was used during this run, since this was known to substantially exceed the thermocouple's time constant. It was determined from the plot that a dwell time of 15 minutes would be sufficient for future runs.

4.2 Temperature Profile

The temperature profile in the furnace was the result of radiation and convection. In particular, assuming a constant temperature on the inside surface of the furnace, examining the view factor, alone, did not explain the observed temperature profile, suggesting that convection

also played a role. A second-order polynomial fit (Equation 3) is illustrated below (Figure 7). The furnace had a region of "constant" temperature (within 1% of the set temperature) that was at least five inches long. The temperature at all depths that were considered fell within 5% of the set temperature of the furnace.

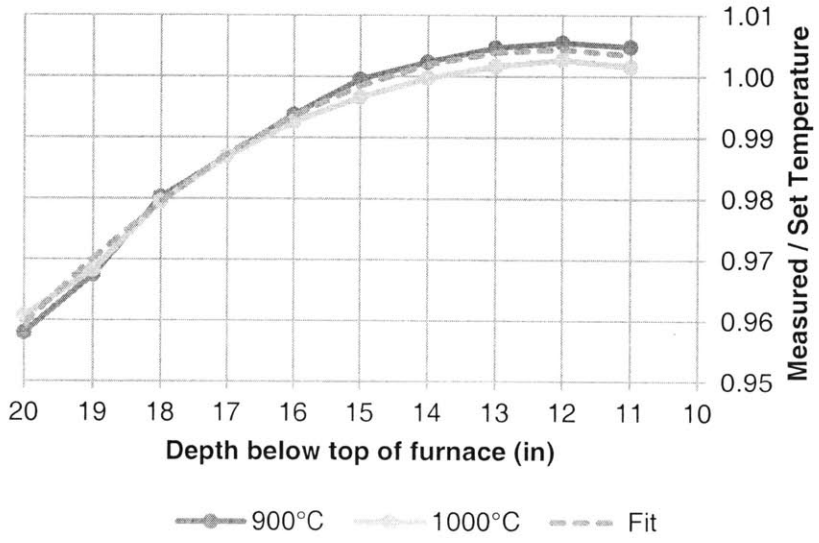

Figure 7: The measured temperature was nearly identical to the set temperature at depths between 13 to 14 inches and within 1% of set temperature at depths between 11 to 16 inches. (All temperatures were measured in Kelvin.)

4.3 Effect of Flow Rate

Flow rate had a minor effect on the measured temperature within the furnace. The temperature in the furnace was measured for two different set temperatures and for four different values of the flow rate. The findings (Figure 8) aligned with the expected result; that is, as the flow rate increased, there was some slight drop in the temperature at the center of the furnace, but the overall effect was nearly negligible. This was expected because at these high temperatures, radiation is the primary mode of heat transfer.

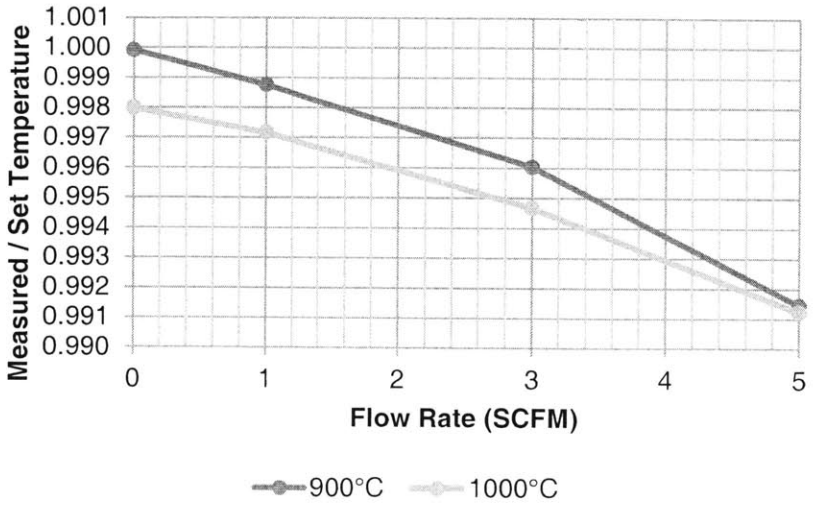

Figure 8: The data illustrated here was collected at a depth of 13 inches. Flow rate has a minor effect on the measured temperature relative to the set temperature. Even at the maximum value of the flow rate allowed by the equipment, the temperature in the tube drops by less than 1%.

4.4 Carrier Lifetime

The measured minority carrier lifetimes in the samples allowed calculation of the amount of iron concentration present. Lifetimes were recorded at an excess minority carrier density (injection level, Δn), value of 3×10^{14} cm^{-3}. Originally, there was much variance in the results, arising from a number of abnormalities in the process. An attempt was made to use a higher Δn value to reduce the noise-to-signal ratio in the measurements, but unfortunately, this was not possible, even after lowering the bulb as low as possible and removing diffusers from the lifetime measurement device.

One phenomenon that was observed was a noticeable difference in measured lifetimes depending on which side of the sample was facing down (Figure 9). "Top" was defined to be the side with the higher carrier lifetime. This phenomenon was also observed in the two control samples. This difference could be the result of differences in surface passivation quality; in this case, the effect would have been introduced during silicon nitride (SiN_x) deposition, either due to SiN_x deposition quality, or since one side of each sample was smoother than the other, producing a longer lifetime. One way to mitigate this phenomenon in the future would be to polish both sides to the same smoothness prior to SiN_x deposition. However, the effect would continue to exist if it were the result of inconsistent SiN_x deposition quality.

The measured carrier lifetimes were used to calculate expected iron concentration (Table 1, Figure 10). "Bottom" and "Top" values were separated for this calculation for consistency;

average values yield results of a similar magnitude for the lifetimes, but higher uncertainties due to the previously described discrepancy. Further experimentation is necessary prior to drawing any conclusions from this section due to the small sample size and aforementioned high variance. The accepted value[6] for solubility of iron in silicon at 766°C is 1.0×10^{12} cm^{-3}.

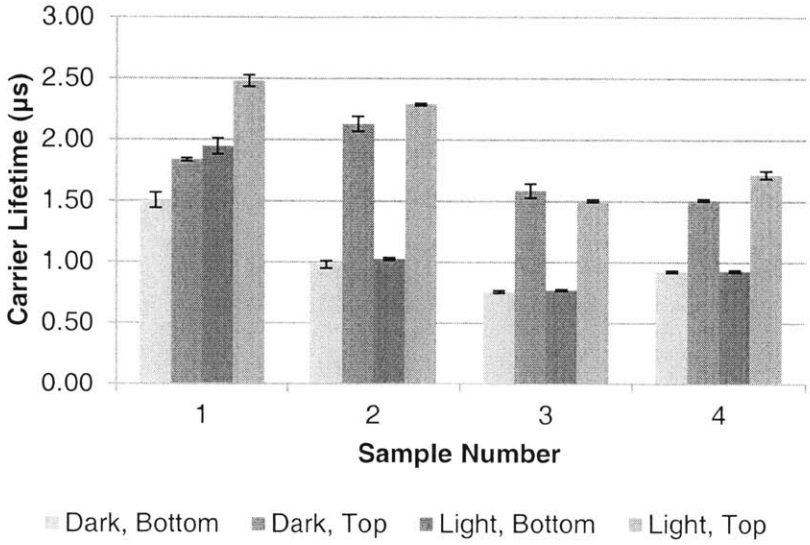

Figure 9: Measured carrier lifetimes (Δn = of 3×10^{14} cm^{-3}). Each sample was measured five times on either side, before and after exposure to light (for a total of 20 measurements per sample). Illustrated uncertainties are 1σ values (normal distribution in measurements was assumed).

Table 1: Data on silicon samples. For carrier lifetimes, a Δn value of 3×10^{14} cm^{-3} was used. Reported lifetimes are the mean of five measurements; iron concentrations are calculated. In each cell, the upper value is the "Top" value, and the lower one is the "Bottom" value. Reported uncertainties are 1σ values (normal distribution in measurements was assumed).

Sample Number	Quench Temp. (°C)	Lifetime, Dark (µs)	Lifetime, Light (µs)	Fe conc. ($\times10^{12}$ cm^{-3})	Notes / Abnormalities
AG1	n/a	10.07 ± 0.09 6.79 ± 0.03	11.50 ± 0.11 10.54 ± 0.13	1.9 ± 0.2 8.1 ± 0.2	Control ("As Grown")
AG2	n/a	7.62 ± 0.01 3.55 ± 0.04	9.17 ± 0.04 5.15 ± 0.04	3.4 ± 0.1 13.6 ± 0.5	Control ("As Grown")
1	766	1.84 ± 0.01 1.50 ± 0.06	2.48 ± 0.05 1.95 ± 0.07	22.0 ± 1.3 23.4 ± 5.0	Fell into furnace; was exposed to air while hot; sat on top of oil; chipped
2	766	2.13 ± 0.06 0.98 ± 0.03	2.29 ± 0.01 1.03 ± 0.01	5.1 ± 2.1 7.1 ± 4.9	
3	766	1.58 ± 0.06 0.76 ± 0.01	1.50 ± 0.01 0.77 ± 0.01	-5.2 ± 3.6 3.7 ± 3.2	Fell outside of oil; chipped
4	766	1.51 ± 0.01 0.92 ± 0.01	1.72 ± 0.03 0.93 ± 0.01	12.4 ± 1.7 1.1 ± 2.5	
5	845	n/a	n/a	n/a	Shattered upon hitting oil
6	845	n/a	n/a	n/a	Broke upon hitting oil
7	845	n/a	n/a	n/a	Sat on top of oil; sensor unable to measure lifetime
8	845	n/a	n/a	n/a	Broke upon hitting oil

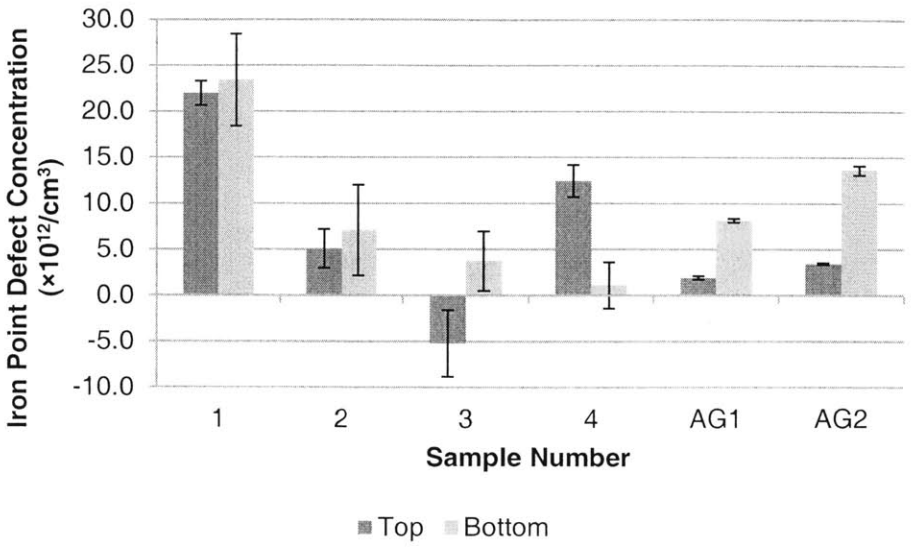

Figure 10: Calculated iron point defect concentrations, based on carrier lifetimes (Δn = of 3×10^{14} cm^{-3}). In this chart, the height of each bar is the calculated iron concentration based on the average of the five measured carrier lifetimes under the corresponding conditions. Illustrated uncertainties are 1σ values (normal distribution in measurements was assumed). Recall that the accepted value[6] for solubility of iron in silicon at 766°C is 1.0×10^{12} cm^{-3}.

Of particular note is the observation that, solely based on these lifetime measurements, the control samples appear to have iron concentrations comparable to the concentrations in the samples in which iron was deliberately introduced. Furthermore, in one case, the calculated iron concentration is negative, and in another case, the 1σ error bars includes negative values for the iron concentration. This raises the possibility of other sources of error that overshadow the effect that this section tried to observe.

Comparing these results against published values[7] suggests a discrepancy between the measured lifetimes and the implied iron concentration in the samples. In particular, here, we attribute the entire change in lifetime is due to the iron concentration, but there may be other metastable defects that are also partially responsible. Other metastable defects would also explain how samples that *should* have an iron concentration of approximately 1.0×10^{12} cm^{-3}, based on the solubility of iron in silicon at 766°C, appear to have much higher concentrations.

Another possible explanation for the observed values is that, due to the quality of the SiN_x deposition, high surface recombination velocities affected the lifetime measurements. Although we are trying to measure the carrier lifetime in the bulk material, τ_{bulk}, we actually measured the effective carrier lifetime, τ_{eff}, which is affected by the surface carrier lifetime, τ_{surf} as described in Equation 4:

$$\frac{1}{\tau_{eff}} = \frac{1}{\tau_{bulk}} + \frac{1}{\tau_{surf}}. \quad (4)$$

In theory, the SiN_x deposition should greatly increase the carrier lifetime at the surface, making the last term of the equation negligible. However, if the last term is non-negligible due to a short surface carrier lifetime, then this would introduce an additional source of error, and possibly variability into the lifetime measurements.

A final explanation for the observed discrepancy in the calculated iron concentration is the high sensitivity of the calculated iron concentration to the measured lifetimes. Indeed, in the case of samples 2, 3, and 4, the uncertainty is of the same order of magnitude as the iron concentration itself. Small changes in measured carrier lifetimes would substantially affect calculated iron concentration; thus, more precise measurements of the carrier lifetimes would improve results.

5. Conclusions

This thesis sought to determine an appropriate dwell time, quantify the relationship between the set temperature and measured temperature within the furnace, determine the effect of flow rate on the temperature within the furnace, and measure the concentration of iron in silicon samples by measuring minority carrier lifetimes. For this thermocouple, 15 minutes was determined to be a sufficient dwell time. The equation $\theta = \left(-7.29\times10^{-4}\right) d^2 + 0.0177d + 0.897$ closely described the temperature profile within the furnace at a flow rate of 1.0 SCFM. Varying flow rate had a negligible effect on the temperature profile within the furnace. Finally, there was a great deal of variance in the carrier lifetimes of the samples that were produced in the furnace due to a number of abnormalities that occurred during processing. Possible sources of error included other metastable defects, surface carrier lifetimes, and high sensitivity of the calculated iron concentration to the measured carrier lifetimes.

Future research done using this equipment will be able to take advantage of this work to estimate accurately what the temperature will be in the furnace at a particular point for a given flow rate. One recommendation to avoid processing abnormalities would be to automate the lowering of the silicon samples into the furnace at the beginning of the quenching process. A second recommendation would be to warm up the oil prior to quenching to avoid breaking samples that have been heated to higher temperatures.

Acknowledgements

The author would like to thank Professor Buonassisi for providing lab equipment and guidance for the research. In addition, the author would like to thank David Fenning for supervision and support, as well as Alexandria Fecych and MIT EH&S for training.

References

1. Incropera, F.P., et. al. "Fundamentals of Heat and Mass Transfer." 6th ed. John Wiley & Sons, Inc., 2007.
2. Macdonald, D.H., Geerligs, L.J., and Azzizi, A. "Iron detection in crystalline silicon by carrier lifetime measurements for arbitrary injection and doping." Journal of Applied Physics, 95(3), pp. 1021-28.
3. "Installation, Operation, & Maintenance Instructions: 1500degG – 1600 degC Tube furnaces, STF & TZF Models." Carbolite, 2003. 19 Dec 2010. http://www.carbolite.com/DocGallery/Mf08%20v3%2719%20-%20STF-TZF.pdf
4. "High Temperature Exotic Thermocouple Probes, Tantalum, Molybdenum, Platinum/Rhodium." Omega Engineering, 2010. 19 Dec 2010. http://www.omega.com/ppt/pptsc.asp?ref=XTA-W5R26
5. "Sinton Instruments – Frequently Asked Questions." Sinton Consulting, Inc., 2009. 19 Dec 2010. http://www.sintoninstruments.com/Sinton-FAQs-LIfetimeTesters-SunsVoc.html
6. "Diffusivity and Solubility of 3d metals." Based on Fuller (1956) and Ortiz (1999). Provided by David Fenning in XLS format, 27 Dec 2010.
7. Istratov, A.A., Hieslmair, H., and Weber, E.R. "Iron Contamination in Silicon Technology." Journal of Applied Physics, A 70, pp.489–534.
8. Green, M.A. "Solar Cells: Operating Principles, Technology, and System Applications." Prentice-Hall, 1982.